# ELECTROLUMINESCENCE IN ANTHRACENE CRYSTALS UNDER TIME VARYING ELECTRIC FIELDS

by

HENRY PETER KUNKEL

A dissertation submitted to the Faculty of Graduate Studies of the University of Manitoba in partial fulfillment of the requirements of the degree of

MASTER OF SCIENCE

© 1975

Permission has been granted to the LIBRARY OF THE UNIVERSITY OF MANITOBA to lend or sell copies of this dissertation, to the NATIONAL LIBRARY OF CANADA to microfilm this dissertation and to lend or sell copies of the film, and UNIVERSITY MICROFILMS to publish an abstract of this dissertation.

The author reserves other publication rights, and neither the dissertation nor extensive extracts from it may be printed or otherwise reproduced without the author's written permission.

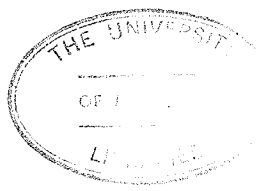

## ABSTRACT

Electroluminescence in anthracene single crystals has been systematically studied, using a sodium electrode as the electron-injecting contact and a silver electrode as the hole-injecting contact, under time varying electric fields at various temperatures. The results show that the electroluminescent brightness decreases monotonically with increasing frequency for the frequency range from 20 Hz to 10 KHz and over the temperature range from -20°C to 40°C. At 10 KHz the electroluminescent brightness is almost undetectable and one-half the period of this frequency has been taken as the time required for the injected carriers to meet each other to produce electroluminescence. In general the brightness increases with increasing temperature, reaches a peak at a critical temperature, and then decreases with increasing temperature. This critical temperature is about 20°C for a.c. fields and about 40°C for half-wave rectified a.c. fields, and this phenomenon is attributed to a smaller space charge created by the a.c. than by the d.c. fields. There is a delay time between the application of the fields and the appearance of electroluminescence, and this delay time decreases with increasing frequency and saturates at a value which is associated with the transit time of the electrons across the sample. The large delay time at low frequencies is associated with the time taken for an electron space charge to build up near the anode to enhance hole injection from the anode.

## ACKNOWLEDGEMENTS

The author wishes to express his sincere appreciation to Dr. K.C. Kao for suggesting this thesis subject and for his supervision of the project.

The author also wishes to extend his sincere thanks to Dr. W. Hwang for his valuable assistance and many discussions.

Sincere thanks are given to the graduate students of the Materials Research Laboratory and the staff of the Electrical Engineering Department of the University of Manitoba for their assistance and co-operation.

Henry P. Kunkel

TABLE OF CONTENTS

LIST OF FIGURES

# CHAPTER I

## INTRODUCTION

Electroluminescence is produced in the bulk of a crystal by the recombination of electrons and holes injected into the crystal from injecting electrodes. In organic semiconductors the recombination of electrons and holes leads to the formation of triplet and singlet excitons. It is the radiative decay of singlet excitons which produces electroluminescence. Anthracene has become a model material upon which a great deal of the work in organic semiconductors has been done. Electroluminescence in anthracene using a pair of double injecting electrodes has been observed by many investigators [14, 18, 30]. A great deal of study has gone into the properties of d.c. electroluminescence. Very little work, however, has been done on the properties of electroluminescence resulting from time varying voltages. It is the purpose of this investigation to determine the frequency and temperature dependence of the electroluminescence. Also, the phase relationship between the electroluminescence and the applied voltage will be investigated.

In Chapters II, III, and IV a review will be presented on the properties of the excitons in anthracene, the processes involved in electroluminescences and the properties of d.c. electroluminescence. Chapter V will describe the experimental procedures involved in this investigation and Chapter VI will present and discuss the results obtained. The conclusions will be given in Chapter VII.

# CHAPTER II

## EXCITONS IN ANTHRACENE

The study of excitons in anthrancene crystals began in 1963 with the discovery that red light from a ruby laser cangenerate detectable concentrations of triplet excitons (mobile neutral electronic excited state of a crystal with spin of 1) in spite of the low probability for this transition [20]. Experimental and theoretical studies of the exciton have subsequently become an active area of research in the field of organic semiconductors. Anthracene has become a model system for these materials upon which a great deal of research has been conducted.

In organic crystals, such as anthracene, weak Van der Waals attractions bind the molecules together. The intermolecular interactions can thus be regarded as a weak perturbation to a non-interacting array of molecules. The electronic energy levels in the crystal are in fact indentifiable with the molecular states. Figure (2.1) shows the electronic energy levels, for the isolated anthracene molecule, from which the exciton bands arise.

In studying the dynamic properties of excitons we need only to consider the lowest singlet and triplet exciton bands since any higher exciton state which is populated, rapidly undergoes a radiationless decay to the lowest state.

A most interesting property of triplet exictons is the mutual annihilation of pairs of triplets resulting in the production of a singlet. The lifetime of singlet excitons in anthracene has been reported to be approximately $10^{-8}$ sec [39, 48]. The characteristic blue flourescence resulting from the decay of directly generated singlets is thus called

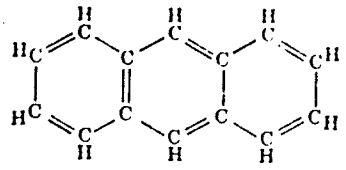

anthracene molecule

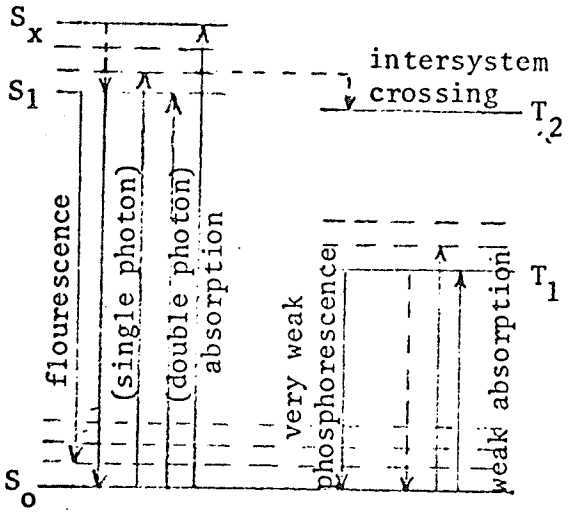


Fig. 2.1 Electronic energy level for anthracene molecule

Excitons in molecular crystals are best described by the Frenkel or tight-binding model of the exciton. A Frenkel exciton is essentially an excited state of a single atom (molecule), but the excitation can hop from one atom (molecule) to another because of the coupling between neighbouring atoms (molecules). The figure shows the electronic energy levels for the isolated anthracene molecule from which the exciton bands arise. The singlet and triplet manifolds are split to sublevels due to molecular vibrations (dashed horizontal lines). The solid lines represent radiative transitions and the dashed non-radiative transitions. In the crystal the $S_o$-$S_1$ energy difference and the $S_o$-$T_1$ energy difference are 3.42 eV and 1.80 eV respectively.

prompt flourescence. The lifetime of the triplet exciton varies from less than a millisecond to 25 m sec depending on the purity of the sample [39, 48]. Thus flourescence resulting from singlets produced by the annihilation of pairs of triplets is delayed by six orders of magnitude longer than the prompt flourescence. This component is called "delayed flourescence". Thus the irradiation of anthracene crystals by light corresponding to the triplet absorption region (14,720 $cm^{-1}$) gives rise to delayed flourescence (25,000 $cm^{-1}$). The triplet exciton concentration is governed by the equation [35]

$$\frac{d[T]}{dt} = G_T - \beta[T] - \gamma[T]^2 \qquad (2.1)$$

where $G_T$ is the exciton generation rate (which for optical experiments is given by $\alpha I$ where $\alpha$ and $I$ are, respectively, the absorption coefficient and illumination intensity) $\beta$ is the unimolecular triplet decay constant and $\gamma$ is the triplet-triplet annihilation rate constant. The singlet exciton concentration $[S]$ is governed by the equation [35]

$$\frac{d[S]}{dt} = -\alpha [S] + \frac{1}{2}\gamma[S]^2 \qquad (2.2)$$

where $\alpha$ is the flourescence rate constant. For low exciton concentrations, $\gamma[T]^2 << \beta[T]$ and under steady state conditions, $\frac{d[S]}{dt} = \frac{d[T]}{dt} = 0$, the intensity of the delayed florescence is

$$I_F = \alpha[S] = \frac{1}{2}\gamma \left(\frac{G_T}{\beta}\right)^2 \qquad (2.3)$$

The intensity of the delayed flourescence is proportional to the square of the triplet exciton generation rate, provided that the triplet concentration is sufficiently low to ensure that the majority of the triplets decay to the ground state by a radiationless monomolecular process. At higher

triplet concentrations, however, bimolecular decay predominates and the delayed flourescence intensity becomes directly proportional to the triplet generation rate.

The flourescence intensity is temperature dependent through the temperature dependence of flourescence reabsorption which, for anthracene, is approximated by the linear relationship [35]

$$R = 10^{7} \ (1 - 7 \times 10^{-3} T) \tag{2.4}$$

Since $\beta$ and $\gamma$ have been shown to be essentially temperature independent by Singh et al. [36], the delayed flourescence should vary with temperature according to equation (2.4). Singh and Lipsett [37], however, have reported that the intensity of flourescence due to triplet-triplet annihilations exhibits an anamolous temperature dependence involving several distinct maxima (Figure 2.2).

To interpret this phenomena Siebrand [35] has developed a kinetic model based on the trapping of triplet excitons. At low temperatures the excitons may become trapped and much of the florescence is due to the annihilation of trapped excitons by free excitons. In general, this would tend to reduce the bimolecular annihilation and also the flourescence intensity. However, if the trapped triplet excitons have a long lifetime as compared to the free excitons then the reverse may occur due to the fact that the annihilation rate is proportional to the square of the triplet lifetime. We denote the concentration of traps of type $i$ and depth $\varepsilon_i$ by $N_i$, the concentration of traps occupied by triplet excitons by $[T_i]$ and the lifetime of the trapped triplets by $\beta_i^{-1}$. The trapping and release rates associated with trap $i$ are given respectively by

$$b_i = Z_i \ (N_i - [T_i]) = P_i - Z_i [T_i]$$

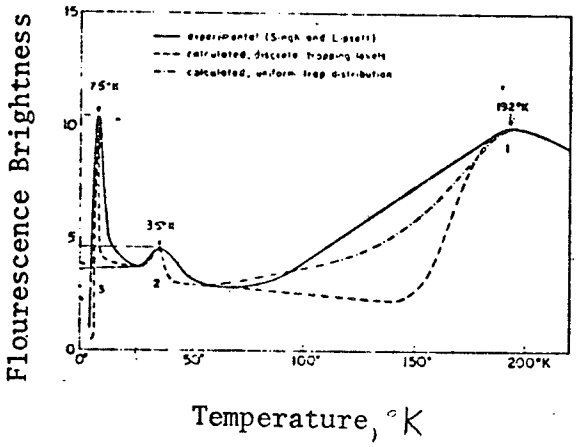


Fig. 2.2 Delayed flourescence as a function of temperature for undoped anthracene crystal. (After Siebrand [34].)

$$q_i = Z_i \, N \exp(-\varepsilon_i/KT)$$

where $Z_i$ is the collision rate between free excitons and traps of type i, which depends on the transport properties of the triplet exciton, and N is the number of molecules per unit volume. Equations (2.1) to (2.3) with trapping become

$$\frac{d[T]}{dt} = \alpha I + \sum_i q_i [T_i] - (\beta + \sum_i P_i - \sum_i Z_i [T_i] + \Sigma \gamma_i [T_i]) \, [T] - \gamma [T]^2 = 0 \qquad (2.5)$$

$$\frac{d[T_i]}{dt} = \alpha_i I + P_i [T] - (q_i + \beta_i + Z_i \, [T] + \gamma_i [T]) \, [T_i] = 0 \qquad (2.6)$$

$$\frac{d[S]}{dt} = - \alpha [S] + \frac{1}{2} \gamma [T]^2 + \frac{1}{2} [T] \sum_i \gamma_i \, [T_i] \qquad (2.7)$$

where $\gamma_i$ is the annihilation rate constant of free and trapped excitons. These equations have been solved by Siebrand [35], for low levels of excitation, with the assumptions that

(1) direct absorption by the traps, that is direct trapped exciton generation, is not important ($\alpha_i = 0$),

(2) the traps are not saturated ($Z_i \, [T] \, [T_i] = 0$),

(3) all bimolecular triplet terms are negligible compared to the unimolecular term, that is, a negligible fraction of the free or trapped triplet excitons decay by triplet-triplet annihilations ($\gamma [T]^2$ and $\gamma_i \, [T] \, [T_i]$ are small), and

(4) The collision cross-section of all trapped triplet excitons are equal.

With the above assumptions equation (2.3) becomes

$$I_F = \frac{1}{2} \gamma \left(\frac{\alpha I}{\beta}\right) B \qquad (2.8)$$

where

$$B = \frac{(1 + \sum_i A_i)}{(1 + \sum_i \rho_i A_i)^2} \tag{2.9}$$

$$A_i = \frac{P_i}{(\beta_i + q_i)} \tag{2.10}$$

$$\rho_i = \frac{\beta_i}{\beta} \tag{2.11}$$

Extrema in the $I_F(T)$ curve occur whenever

$$\frac{dB}{dt} = 0 \qquad \text{or}$$

$$\sum_i A_i' \left[1 + \sum_i \rho_i A_j - 2\rho_i \left(1 + \sum_i A_j\right)\right] = 0 \tag{2.12}$$

where $A_i' = \frac{dA_i}{dT}$. $A_i'$ goes to zero in two limiting situations: at relatively high temperatures where $q_i >> P_i$ and the traps are ineffective and at relatively low temperatures where $q_i << \beta_i$ and the trapped exciton decays before it can escape. If the traps are a set of energetically well separated discrete levels we can expect temperature regions where all $A_i'$ are zero to alternate with regions where all but one $A_i'$ are zero. For a range of finite $A_i'$ equation (2.12) demands that

$$1 + \sum_i \rho_j A_j - 2 \rho_i \left(1 + \sum_j A_j\right) = 0$$

or

$$\rho_i = \frac{(1 + \sum_j{}' \rho_j A_j)}{2 + A_i + 2\sum_i A_j'} \tag{2.13}$$

where the prime on the summation indicates the term $j=i$ is omitted. Combining equations (2.13) and (2.9) we have

$$B^{i}_{ext} = [4\rho_i^{\,2} (1 + \sum_{j}{}' A_j)]^{-1} \tag{2.14}$$

All traps with $j > i$ are empty so that $A_{j>i} \simeq 0$. All traps with $j<i$ are filled and therefore $A_{j<i} \simeq \rho_j/\beta_j$. For the special case where only one trapping level is operative equations (2.13) and (2.14) reduce to

$$\rho_1 = (2 + A_1)^{-1} \tag{2.15}$$

$$B_{extr} = [4\rho_1 (1 - \rho_1)]^{-1} = \beta^2/4\beta_1 (\beta - \beta_1) \tag{2.16}$$

Since $A_1 > 0$ we can conclude from equation (2.15) that $\beta_1 < \frac{1}{2}\beta$. It follows that for the case of a single trapping level B has a maximum if the lifetime of the trapped triplet exciton is more than twice the lifetime of the free exciton. Similar arguments apply to the more general case described by equations (2.13) and (2.14). The two limiting conditions for $A_i' = 0$ result in two minima whenever equation (2.14) gives rise to a maximum. From equation (2.14) it is also seen that the relative heights of the maxima should be an increasing function of temperature unless the triplet lifetime is longer for the shallower traps. This is because of the monotonic decrease of $\Sigma A_j$ with temperature.

Siebrand's analysis completely describes every discrete trap with three parameters $\epsilon_i$, $N_i$ and $\beta_i$ which can be obtained from the $I_F[T]$ curve by means of equations (2.12) to (2.14). With the proper choice of parameters Siebrand [35] has been able to approximately reproduce the experimental results of Singh and Lipsett using a three discrete trap model (the solid curve of Figure 2.2). Siebrand has obtained a better agreement by assuming a diffuse trap distribution for the high temperature

trap. This result is shown in the dot-dash line in Figure 2.2. The discrepancy that remains could indicate that there are more than three discrete (distributed) traps.

In his theory Siebrand assumed that all triplet-triplet annihilations contributed to the formation of flourescing singlet states. If all triplet spin states occur with equal probability, however, no more than one collision in nine can lead to a singlet. Goode and Lipsett [11] have therefore replaced that total annihilation rates $\gamma$ and $\gamma_i$ by radiative annihilation rates $f\gamma$ and $f'\gamma_i$, where $f\gamma$ is the component of the free triplet annihilation rate $\gamma$ and $f'\gamma_i$ is the component of the free-trapped annihilation rate $\gamma_i$ that lead to the formation of florescing states. Since the collision rate restricts the magnitude of the annihilation rate, we have that $Z_i > \gamma_i \geq f'\gamma_i$ where $Z_i \geq qf'\gamma_i$.

Goode and Lipsett [11] have studied the relationship between delayed florescence and excitation intensity at low temperature and have found deviations from the square law at comparatively low excitation intensities. To account for the deviations from the square law Goode and Lipsett have extended the theory of Siebrand to include the saturation of triplet traps (the term $Z_i[T][T_i]$) as well as the depopulation of free and trapped triplets by bimolecular annihilation (the terms $\gamma_i[T][T_i]$ and $\gamma[T]^2$). The expression obtained gives a reasonable agreement with the experimental results.

At room temperature the triplet traps are not effective and the square law deviation is due to free exciton annihilation only. Thus, for small exciton concentrations the deviation is negligible as expected.

Figure 2.3 gives a detailed description of the exciton transitions possible in organic crystals. The solid lines represent radiative transitions and the dashed lines represent non-radiative transitions. It is assumed that the singlet and triplet excitons have generation rates of $G_S$ and $G_T$ respectively. The singlet and triplet excitons have the rate constants $\alpha_1$ and $\beta_1$, respectively, for the radiative transitions to the ground state with the emission of photons. The rate constants for the non-radiative transitions with the emission of phonons is given by $\alpha_2$ and $\beta_2$. Singlet and triplet excitons may relax into traps at a level $\epsilon_t$ lower in energy with the rate constants $\alpha_i$ and $\beta_i$ respectively. Trapped excitons may be thermally detrapped and then decay radiatively with the rate constant $\alpha_{i1}$ and $\beta_{i1}$ and non-radiatively with the rate constants $\alpha_{i2}$ and $\beta_{i2}$ for the singlet and triplet excitons, respectively. The effective rate constant for triplet-triplet annihilation is given by $\gamma$ and that for triplet-trapped triplet annihilation is given by $\gamma_i$. The rate constant for the production of singlet excitons from the triplet-triplet annihilation (triplet-triplet annihilation may lead to a higher energy triplet) is given by $f\gamma$ and from triplet-trapped triplet annihilation by $f'\gamma_i$. The singlet exciton (S) may also make a transition to the triplet state ($T_1$) via a higher energy triplet state ($T_2$). This is referred to as intersystem crossing. Adolf et al. [1] have shown that this process is neglegible compared to the radiative decay of singlet excitons. Siebrand et al., in their analysis of the temperature dependence of the delayed flourescence in anthracene, have also assumed that the non-radiative decay mechanism of singlet and triplet excitons, as well as the prescence of singlet traps, can be ignored.

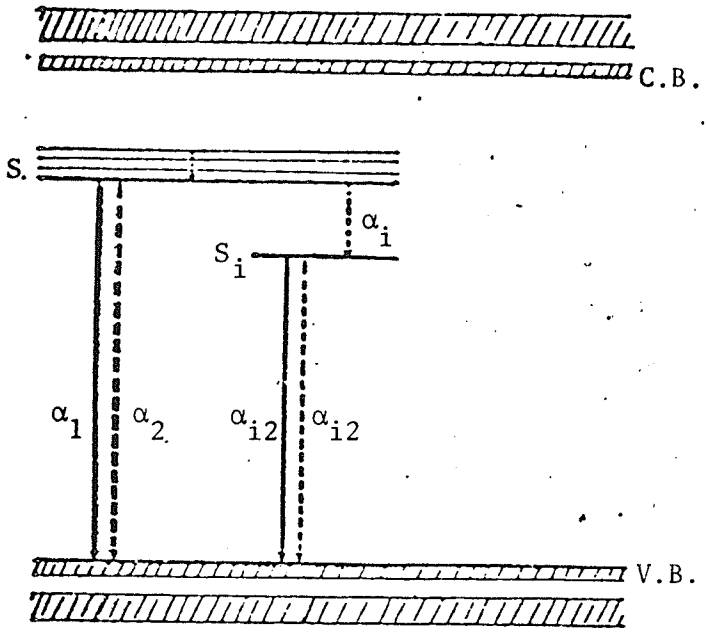


(a)

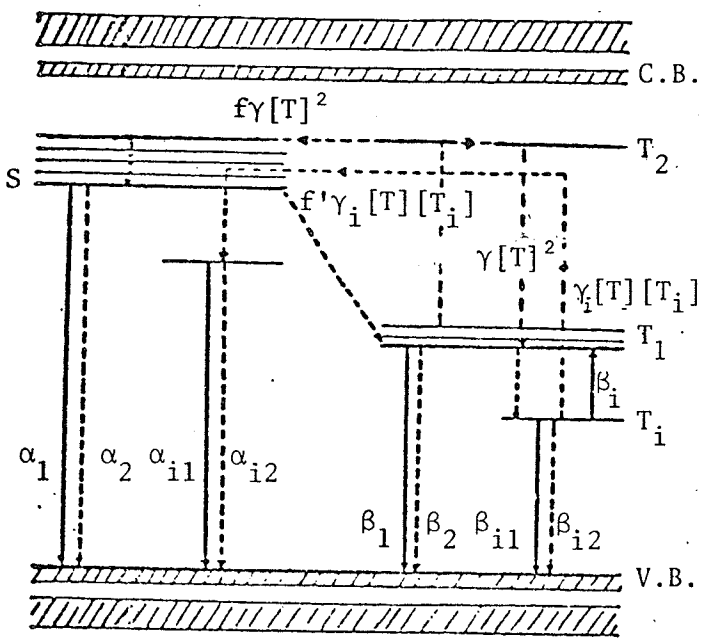


(b)

Fig. 2.3 Exciton transitions in organic crystals. Solid lines, radiative transition; dashed lines, non-radiative transition.
(a) prompt flourescence
(b) delayed flourescence

# CHAPTER III

# ELECTROLUMINESCENCE

Electroluminescence is produced in the bulk of a crystal by direct recombination of electrons and holes injected into the crystal from injecting electrodes. Electron-hole recombination may lead to both radiative and non-radiative transitions. It is generally accepted [14] that the recombination of injected holes and electrons in organic semiconductors will yield singlet and triplet excitons and the electroluminescence is produced by the radiative decay of the singlet excitons. The quantum yield of electroluminescence will depend on the probability of radiative and non-radiative transitions and on the efficiency of producing the radiative exciton. In this chapter we will discuss the mechanisms of electroluminescence and also the dominant non-radiative transitions of the exciton.

## 3.1 Electron-hole Recombination

Electron-hole recombination involves two steps. First the electron and hole must come close enough to one another to be trapped by the other's coulomb field. This can occur in a radius around the carriers given by [16]

$$r_{kT} = \frac{2e^2}{3\epsilon kT} \tag{3.1}$$

A carrier within this sphere must loose sufficient energy through scattering to become trapped. For this to occur the mean free path of the carrier must be small compared to the radius $r_{kT}$ the Coulomb capture radius. For anthracene $\epsilon = 3.14\ \epsilon_o$ and $r_{kT} = 120\ \text{Å}$ at room temperature. The mean free path of the carriers in anthracene is only

a few lattice parameters [14, 26]. Thus the rate determining process for electron-hole recombination is the diffusion of oppositely charged particles toward each other. This satisfies the conditions for which Langevin's theory of carrier recombination applies [26]. The relative drift velocity of a positive and negative charge when they are a distance r apart is

$$V_d = (\mu_+ + \mu_-) \frac{q}{\varepsilon r^2} \tag{3.2}$$

where $\mu_+$ and $\mu_-$ are the drift mobilities of the positive and negative charges respectively. The recombination rate will be the flow rate of positive charges into a sphere of radius r around a negative charge. Thus, the recombination rate is

$$K = 4\pi r^2 \varepsilon V_d = 4\pi q (\mu_+ + \mu_-) \tag{3.3}$$

If we take $\mu_+ + \mu_- \simeq 2\ cm^2\ V^{-1}\ sec^{-1}$ the recombination rate will be $1.2 \times 10^{-6}\ cm^2\ V^{-1}\ sec^{-1}$. This compares very well with experimentally determined values [38].

The recombination of electrons and holes in organic semiconductors will yield singlet and triplet excitons. It is generally assumed that

(1) the rates of production of singlet and triplet excitons is proportional to the multiplicities of the state, that is three times as many triplets as singlets are generated, and

(2) the annihilation of a pair of triplets can produce either an electronically or vibronically excited triplet exciton or a singlet exciton. Since three times as many pairs of excitons have total spin one than have a total spin of zero, this suggests that triplet-triplet annihilations will produce three times more triplets than singlet excitons. The kinetics of the above model can be described by

$$4(e+h) \rightarrow 1S + 3T \tag{3.4}$$

$$8T \rightarrow 1S + 3T^{*} \tag{3.5}$$

Since any excited triplet state decays back to the lowest triplet state in a time much shorter than the lifetime of the latter, reaction (3.5) becomes

$$5T \rightarrow 1S \tag{3.6}$$

Combining equations (3.4) and (3.6) gives

$$20(e+h) \rightarrow 5\ S_{dir} + 15T \rightarrow 5\ S_{dir} + 3\ S_{ind} \tag{3.7}$$

where e and h represent the electron and hole and S and T the singlet and triplet excitons respectively.

## 3.2 Exciton-Carrier Interactions

Quenching of delayed flourescence by injected carriers is observed when either monomoledulor or bimoleculor exciton processes are the dominant exciton-decay mechanism. With small triplet exciton densities, injected carriers reduce the triplet lifetime and hence the delayed floure-scence intensity [42, 43, 13]. Figure 3.1 shows the variation of the triplet exciton lifetime with injected free carrier densities as obtained by Wakayama and Williams [43]. If the carriers are not trapped then the triplet lifetime $\tau$ will obey the relation

$$\frac{1}{\tau} - \frac{1}{\tau_o} = kn \tag{3.8}$$

where $n = \frac{3}{2}\ \varepsilon\varepsilon_o\ \frac{V}{eL^2}$ is the carrier density, $\tau_o$ is the triplet lifetime in the absence of any injected carriers and k is the exciton-carrier interaction rate constant. When the triplet density is large, however,

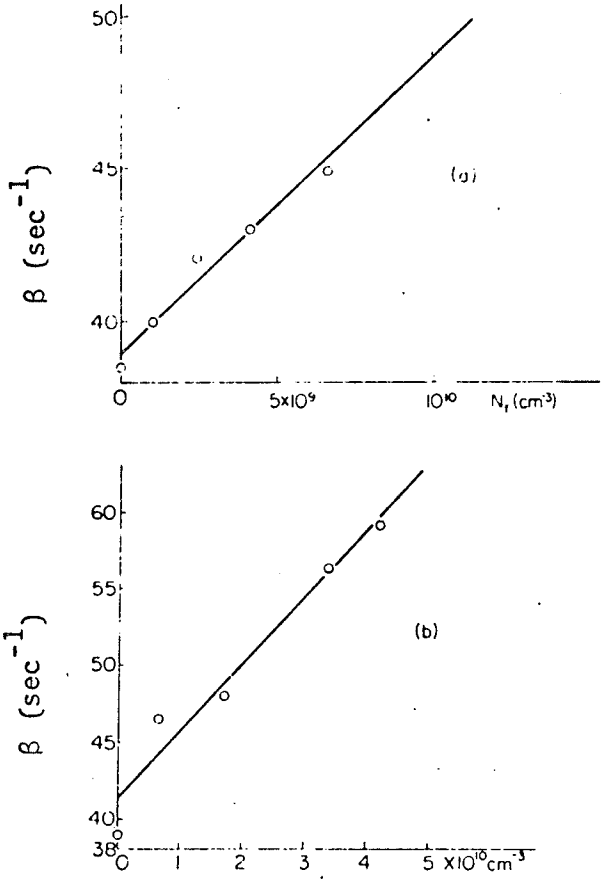


Fig. 3.1 The triplet exciton lifetime as a function of injected free carrier density for (a) holes and (b) electrons at room temperature. (After Wakayama and Wilfliams [43].)

this reduction in triplet lifetime becomes ineffective. The delayed flourescence intensity does, however, decrease in the presence of injected carriers. Wakayama and Williams [43] have shown that the interaction of charge carriers with the singlet exciton produced by triplet-triplet annihilation cannot satisfactorily explain this drop in flourescence intensity. Thus in the case of high triplet concentrations the most significant effect of the presence of charge carriers is not on either the triplet or singlet exciton, but rather on some intermediate state.

The formation of a triplet pair state during the triplet annihilation process has been suggested by several studies [40]. Wakayama and Williams have developed the following kinetic model which uses this pair state to account for the flourescence quenching. K(N) represents the interaction rate constant between the carriers and the pair states.

$$T + T \underset{K_{-1}}{\overset{K_1}{\leftrightarrow}} |TT\rangle \begin{cases} \xrightarrow{K_{2S}} S \xrightarrow{K_3} S_o \\ \xrightarrow{K_{2T}} T \\ \xrightarrow{K(N)} 2S_o \end{cases} \qquad (3.9)$$

The triplet pair state $|TT\rangle$ consists of two triplet excitons which are close enough to interact. K(N) can be expressed in terms of the interaction cross section, $\sigma$, between the carrier and the intermediate state, their thermal velocities $u$ and $\nu$ respectively and the ratio of free to total carrier density, $\theta$. [43]

$$\begin{aligned} K(N) &= \nu N_t (1 - \theta)\sigma + \theta N_t \sigma (u + \frac{\nu^2}{3u}) \qquad u > \nu \\ &= \nu N_t (1 - \theta)\sigma + \theta N_t \sigma (\nu + \frac{u^2}{3\nu}) \qquad u < \nu \end{aligned} \qquad (3.10)$$

$\theta$ varies from 1 to $10^{-4}$ depending on crystal purity.

Wakayama and Williams have been able to account for the observed flourescence quenching using the pair state model.

The fact that quenching of delayed flourescence by injecting carriers is observed indicates that exciton carrier interactions will affect the quantum efficiency of electroluminescence.

## 3.3 Exciton-surface Interactions

The interaction of excitons with a crystal surface may result in the quenching of the exciton. The quenching mechanism at the boundary between an organic semiconductor and an electrode consists of either a charge transfer or an energy transfer process. An exciton can transfer an electron to a trapping centre at the surface producing a free hole in the semiconductor or an exciton can transfer its energy to the acceptor molecules present at the surface.

Williams, Adolf and Schneider [45] have measured the monomolecular decay constant, $\beta$, as a function of crystal thickness. After excitation by a helium-neon laser the exciton lifetime ($\beta^{-1}$) was determined from the relationship $I_F \alpha \exp(\frac{2t}{\tau})$, where $\tau$ is the triplet lifetime. The crystal thickness was found to have a large effect on the triplet lifetime. Figure 3.2 shows the result as obtained by Williams et al.

The concentration of triplet excitons in a thick crystal may be described by

$$\frac{d[T]}{dt} = - \beta[T] + \gamma[T]^2 \qquad (3.11)$$

where as before $\beta$ is the unimolecular triplet decay constant and $\gamma$ is the bimolecular triplet decay constant. If the decrease in triplet lifetime experimentally observed is due to diffusion of excitons to the surface followed

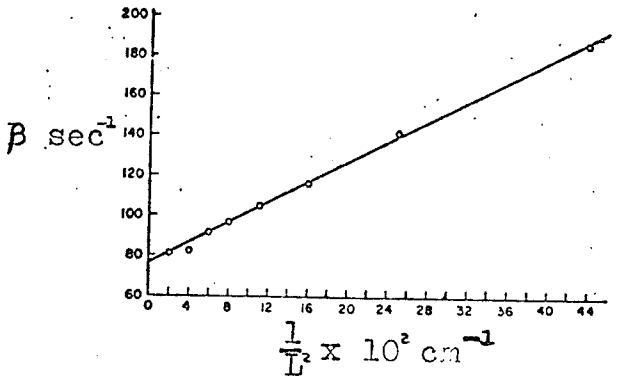


Fig. 3.2 The monomolecular triplet decay constant as a function of $1/L^2$. L is the crystal thickness. (After Williams et al [45].)

by surface quenching then equation (3.11) becomes

$$\frac{d[T]}{dt} = - \beta[T] - \gamma[T]^2 + D \frac{d^2[T]}{dx^2} \tag{3.12}$$

where $D$ is the diffusion constant in the $x$ direction. Assuming complete surface quenching (that is $[T\ (x = 0, L)] = 0$), weak excitation and a uniform initial triplet density ($[T\ (t = 0, x)]$ = constant), the solution of equation (3.12) was shown by Kepler and Switenelick [21] to be

$$[T\ (x, t)] = \frac{4}{\pi} [T]_o \sum_{k=o}^{\infty} \frac{1}{2k+1} \exp \{-[\beta + \frac{(2k+1)^2 \pi^2 D}{L^2}]t\} \sin \frac{2k+1}{L} \pi x \tag{3.13}$$

where $L$ is the crystal thickness and $\beta'$ the reciprocal of the actual lifetime. For time large enough

$$[T] = \frac{4}{\pi} [T]_o \exp (-\beta' t) \sin (\frac{\pi x}{L}) \tag{3.14}$$

where

$$\beta' = \beta + \frac{\pi^2 D}{L^2} \tag{3.15}$$

since the $k=o$ term dominates. The reciprocal lifetime has been plotted as a function of $\frac{1}{L^2}$ in Figure (3.2). It should be noted that the diffusion constant of the triplet exciton can be obtained from the slope of the curve. It should also be noted that a change in triplet lifetime from the bulk value first becomes apparent with a crystal thickness of 750-1000μ. For crystals thicker than this surface quenching of triplet excitons can be ignored.